

## Atomic force microscopy measurement of the Young's modulus and hardness of single LaB<sub>6</sub> nanowires

Han Zhang,<sup>1</sup> Jie Tang,<sup>1</sup> Lin Zhang,<sup>2</sup> Bai An,<sup>2</sup> and Lu-Chang Qin<sup>3,a)</sup>

<sup>1</sup>*ID Nanomaterials Research Group, National Institute for Materials Science, Sengen 1-2-1, Tsukuba, Ibaraki 305-0047, Japan*

<sup>2</sup>*National Institute of Advanced Industrial Science and Technology (AIST), Higashi 1-1-1, Tsukuba, Ibaraki 305-8565, Japan*

<sup>3</sup>*W.M. Keck Laboratory for Atomic Imaging and Manipulation, Department of Physics and Astronomy, University of North Carolina at Chapel Hill, Chapel Hill, North Carolina 27599-3255, USA; Curriculum in Applied and Materials Sciences, University of North Carolina at Chapel Hill, Chapel Hill, North Carolina 27599-3255, USA*

(Received 16 October 2007; accepted 14 April 2008; published online 2 May 2008)

We have employed the atomic force microscopy based (a) three-point bending and (b) nanoindentation methods to obtain the Young's modulus and hardness of single LaB<sub>6</sub> nanowires. The Young's modulus,  $E=467.1 \pm 15.8$  GPa, is the same as that of the LaB<sub>6</sub> single crystals but larger than the sintered polycrystalline LaB<sub>6</sub> samples. The nanoindentation hardness of the LaB<sub>6</sub> nanowire is  $H=70.6 \pm 2.1$  GPa at an indent depth of 4.6 nm, which is higher than that of the LaB<sub>6</sub> single crystals, LaB<sub>6</sub> polycrystals, and W metals. A superior resistance against thermal vibration, field modification, and ion bombardment is expected for the LaB<sub>6</sub> nanowires as a field-emission point electron source. © 2008 American Institute of Physics. [DOI: 10.1063/1.2919718]

LaB<sub>6</sub> nanowires have shown a great potential to replace the W emitter for use as a field-emission point electron source in electron optical instruments, such as the scanning electron microscope (SEM), transmission electron microscope, and the scanning transmission electron microscope.<sup>1</sup> The stability of the emission current is one of the most important performance parameters for a field-emission point electron source. The mechanical properties, such as the Young's modulus and hardness, of a nanowire field emitter have great influence on its emission current stability through their impact on the resistance against thermal vibrations,<sup>2,3</sup> field-induced shaping effect, and ion bombardment.<sup>4,5</sup> While the Young's modulus and hardness have been well documented for the bulk LaB<sub>6</sub> materials, there is no data available for the LaB<sub>6</sub> nanowires in the literature.<sup>4,6</sup> Our recent synthesis of single crystalline LaB<sub>6</sub> nanowires has made such materials available for this type of study.<sup>1</sup> On the other hand, in recent years, atomic force microscopy (AFM) has been demonstrated as a powerful tool in probing the mechanical properties of one-dimensional nanostructures due to its combined capabilities of imaging, direct force measurement, and nanoscale manipulation.<sup>7-14</sup> In this work, we employed the techniques of nanoscale three-point bending and nanoindentation to obtain the Young's modulus and the hardness of single LaB<sub>6</sub> nanowires. These two mechanical properties were also obtained by using the nanoindentation method on several other electron emitter materials, including LaB<sub>6</sub> single crystals, sintered LaB<sub>6</sub> polycrystals, and W metals for comparison.

The LaB<sub>6</sub> nanowires were first grown on a silicon substrate and then transferred onto a silicon wafer which was prepatterned by photolithography to have SiO<sub>2</sub> trenches and holes fabricated with a depth of about 900 nm and widths of between 2 and 5 μm. A single LaB<sub>6</sub> nanowire sitting across a trench/hole is located with an SEM, and then the two sup-

porting ends of the nanobridge were fixed by depositing a layer of W metal using a focused ion-beam system (FIB) to prevent slippage during the force loading. Figure 1(a) shows an AFM topographic image of such a nanobridge. Before the three-point bending measurement, the original sharp AFM probe tip was modified by FIB milling to produce a "tooth" shape with a dent width of about 150 nm in order to secure a firm grip of the nanowire during the force loading, as shown in Fig. 1(b). The AFM probe cantilever has a spring constant of 2.138 N/m as calibrated using a standard calibration cantilever.<sup>15</sup> The single crystalline LaB<sub>6</sub> nanowires have rectangular cross sections, as shown in Fig. 1(c), which is a typical SEM image of the LaB<sub>6</sub> nanowires. For the nanobridge examined in this particular case, the length  $L$ , width  $w$ , and thickness  $t$  were also measured:  $L=4.6$  μm,  $w=100$  nm, and  $t=100$  nm. It is crucial in this measurement to vertically apply the force load on the top of the nanobridge because the force values are calculated using the spring constant for the vertical bending of the cantilever only. The force diagrams drawn in Fig. 1(d) illustrate five circumstances that might occur when the probe tip is placed in the vicinity of the nanowire. The slopes of the force-deflection ( $F$ - $D$ ) curves obtained in these scenarios are in the following sequence: the greatest (I), the smallest (II), the second greatest (III), the smallest (IV), and the greatest (V), depending on if it is the silicon substrate (I and V), the side surfaces of the nanobridge (II and IV) or the top surface of the nanobridge (III) that is pressed by the probe tip. In Fig. 1(e), the experimentally measured slopes are plotted against the probe tip positions. We can therefore determine that point III in the graph is the slope obtained when the probe tip vertically presses on the top surface of the nanowire. By using the same criteria, the midspan of the nanobridge, indicated by the blue arrow in Fig. 1(a), and a section of the nanowire on the trench top, indicated by the red arrow in the same image, are loaded with the AFM probe tip to obtain the  $F$ - $D$  curves given in Fig. 1(f) in blue and red, respectively. The slope of

<sup>a)</sup>Electronic mail: lcqin@physics.unc.edu.

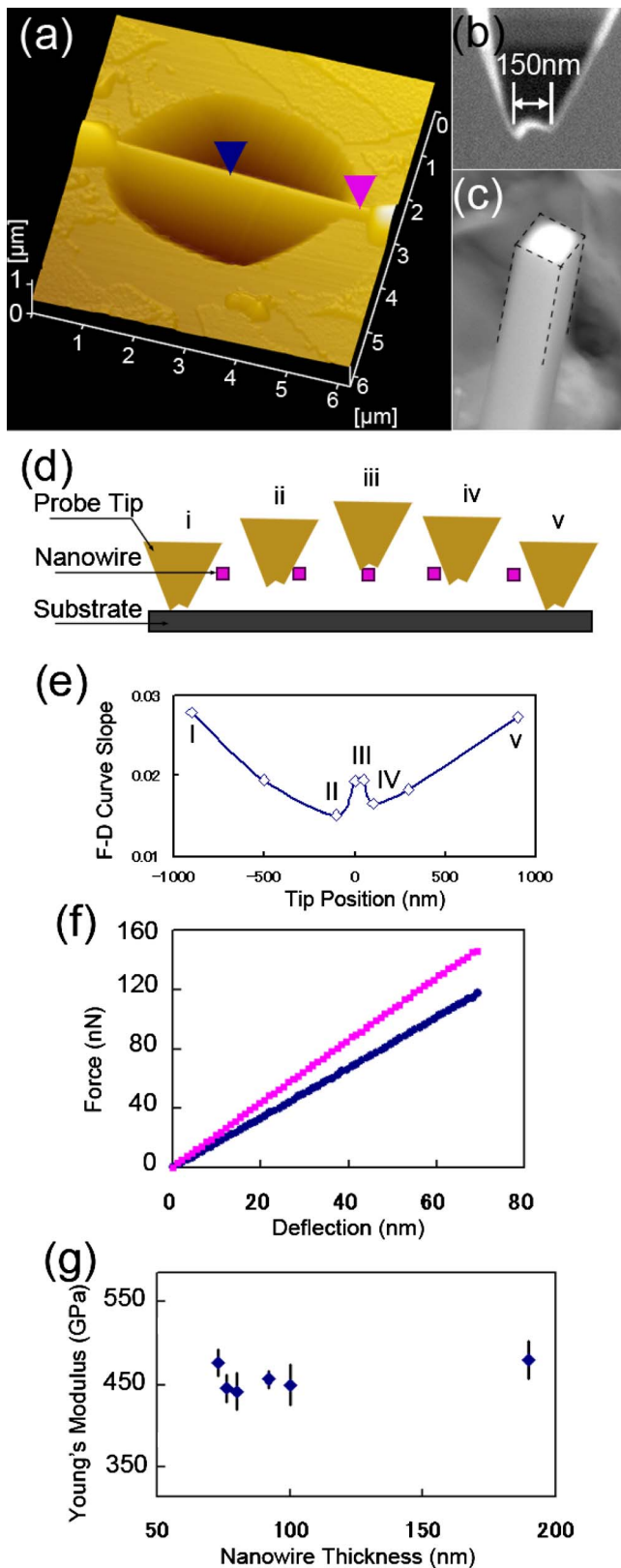


FIG. 1. (Color online) (a) AFM topographic image of a LaB<sub>6</sub> nanowire-bridge with its two ends fixed to the SiO<sub>2</sub> trench top by depositing a layer of W metal. (b) A silicon AFM probe tip modified by FIB to form a “tooth” structure with a 150 nm wide dent for ensuring good grips of the nanowire during force loading. (c) SEM image revealing the rectangular cross section of an individual LaB<sub>6</sub> nanowire. (d) Force diagrams illustrating five circumstances where the probe tip is in the vicinity of the nanowire during force loading. (e) Slopes of the force-deflection curves corresponding to the five circumstances labeled I to V in (d). (f) Force-deflection curves obtained by force loadings at the midspan of the nanowire (blue) and a section on the solid trench top (red). (g) Young’s modulus for six similar structures plotted against the thickness of each tested LaB<sub>6</sub> nanowire.

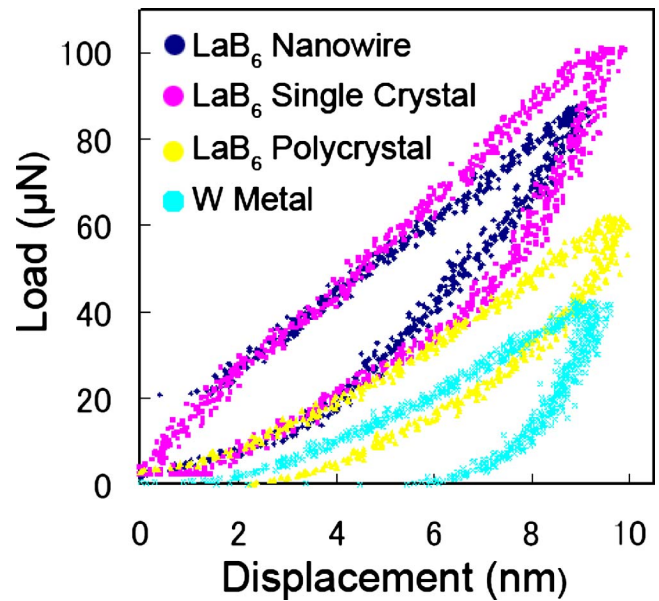


FIG. 2. (Color online) Nanoindentation loading cycles performed on the surface of LaB<sub>6</sub> nanowire (blue), LaB<sub>6</sub> single crystal (red), sintered polycrystalline LaB<sub>6</sub> chip (yellow), and W metal (azure). The LaB<sub>6</sub> nanowire shows the highest hardness.

the blue curve reflects the total spring constant  $K_t$  combining both the spring constant of the cantilever  $K_c$  and the bending spring constant of the nanobridge  $K_n$ , while the slope of the red curve reflects only the spring constant of the cantilever  $K_c$ , where  $K_n = K_t K_c / (K_c - K_t)$  according to the combination law for two springs connected in series. Analogous to the three-point bending test on a beam of rectangular cross section, the Young’s modulus of the nanowire  $E$  can be expressed as  $E = K_n L^3 / (192I)$ , where  $I$  is the second moment of inertia of the nanobridge, which is determined by the geometry of the cross section as  $I = wt^3 / 12$ .<sup>16</sup> After substituting the values for  $K_n$ ,  $L$ ,  $w$ , and  $t$ , we obtained the value of the Young’s modulus  $E = 444$  GPa for this LaB<sub>6</sub> nanobridge under test. Six other similar LaB<sub>6</sub> nanobridges were also examined by the same method and their Young’s moduli  $E$  are plotted against their thickness  $t$  in Fig. 1(g). All six  $E$  values are evenly distributed around an average value of  $467.1 \pm 15.8$  GPa and no obvious size dependence was observed. The Young’s modulus of the LaB<sub>6</sub> nanowire measured by this method equals to that of the LaB<sub>6</sub> single crystals reported in the literature.<sup>6</sup>

To measure the hardness of the LaB<sub>6</sub> nanowires, we applied the nanoindentation method. The LaB<sub>6</sub> nanowires were first transferred onto the polished surface of a silicon wafer. A nanoindenter (Hysitron TriboScope) in conjunction with an AFM (Digital Instruments Nanoscope IIIa) was used for performing both imaging and nanoindentation. We selected a single LaB<sub>6</sub> nanowire on the silicon substrate of thickness  $t = 100$  nm and width  $w = 158$  nm for the nanoindentation measurement. A piece of LaB<sub>6</sub> single crystal [Denka Inc., (001) orientation], a piece of sintered polycrystalline LaB<sub>6</sub> chip (Furuchi Chemistry Inc., 99% in purity), and a piece of W metal foil (Nilaco Inc., 99.95% in purity) were also measured for comparison.

The indentation loading/unloading cycles performed on the LaB<sub>6</sub> nanowire, the LaB<sub>6</sub> single crystal, the LaB<sub>6</sub> polycrystal, and the W metal are all plotted in Fig. 2 in the colors of blue, red, yellow, and azure, respectively. The procedure

TABLE I. Young's modulus  $E$  and hardness  $H$  measured with nanoindentation on samples of single-crystalline LaB<sub>6</sub> nanowire, LaB<sub>6</sub> single crystal, polycrystalline LaB<sub>6</sub> chip, and W metal.

Sample	$E$ (GPa)	$H$ (GPa)
LaB <sub>6</sub> nanowire	439.4 ± 26.4	70.6 ± 2.1
LaB <sub>6</sub> single crystal	428.4 ± 25.7	31.5 ± 1
LaB <sub>6</sub> polycrystal	185.2 ± 11.1	12.3 ± 0.4
W single crystal	436.6 ± 26.2	8.6 ± 0.3

described by Oliver and Pharr were adopted to obtain the Young's modulus  $E$  and the hardness  $H$ .<sup>17</sup> The calculated  $E$  and  $H$  values for these four materials are tabulated in Table I. It shows again that, within the uncertainty of measurement, the  $E$  value for the LaB<sub>6</sub> nanowire equals to that of the LaB<sub>6</sub> single crystal. On the other hand, the LaB<sub>6</sub> nanowire has the highest hardness  $H$  among all four tested materials and this is attributed to the defect-free crystal structure of the LaB<sub>6</sub> nanowires.<sup>1</sup> The LaB<sub>6</sub> polycrystal shows the lowest  $E$  and  $H$  values among all the three forms of LaB<sub>6</sub> tested in this study, which is attributed to the existence of grain boundaries and sintering voids. The W metal has the smallest hardness.

In conclusion, using an AFM-based three-point bending experiment, we have obtained the Young's modulus of single LaB<sub>6</sub> nanowires  $E=467.1 \pm 15.8$  GPa, which equals to that of LaB<sub>6</sub> single crystals reported in the literature.<sup>6</sup> This result is also in agreement with data measured using nanoindentation. The nanoindentation hardness of the LaB<sub>6</sub> nanowire is  $H=70.6 \pm 2.1$  GPa at an indent depth of 4.6 nm, which is higher than that of the LaB<sub>6</sub> single crystals, LaB<sub>6</sub> polycrystals, and W metals. It suggests that, compared to the other conventional electron emitter materials, the LaB<sub>6</sub> nano-

wire field emitter has the largest resistance against thermal vibrations, field modification, and ion bombardment. As a result, a higher stability of electron emission and longer service life are expected using the LaB<sub>6</sub> nanowires.

This work is partially supported by JSPS Grants-in-Aid for Scientific Research No. 19710101 and the "Nanotechnology Network Project" of the Ministry of Education, Culture, Sports, Science and Technology (MEXT), Japan.

<sup>1</sup>H. Zhang, J. Tang, Q. Zhang, G. Zhao, G. Yang, J. Zhang, O. Zhou, and L.-C. Qin, *Adv. Mater. (Weinheim, Ger.)* **18**, 87 (2006).

<sup>2</sup>S. T. Purcell, P. Vincent, C. Journet, and V. T. Binh, *Phys. Rev. Lett.* **88**, 105502 (2002).

<sup>3</sup>M. M. J. Treacy, T. W. Ebbesen, and J. M. Gibson, *Science* **381**, 678 (1996).

<sup>4</sup>V. V. Morozov, V. I. Malnev, S. N. Dub, P. I. Loboda, and V. S. Kresanov, *Inorg. Mater.* **20**, 1225 (1984).

<sup>5</sup>J. F. Hainfeld, *Scan Electron Microsc.* **1**, 591 (1977).

<sup>6</sup>K. M. Winter, D. Lenz, H. Schmidt, S. Ewert, S. Blumenroder, E. Zirmgiebl, and K. Winzer, *Solid State Commun.* **59**, 117 (1986).

<sup>7</sup>E. P. S. Tan and C. T. Lim, *Compos. Sci. Technol.* **66**, 1102 (2006).

<sup>8</sup>J.-P. Salvetat, G. A. D. Briggs, J.-M. Bonard, R. R. Bacsá, A. J. Kulik, T. Stöckli, N. A. Burnham, and L. Forró, *Phys. Rev. Lett.* **82**, 944 (1999).

<sup>9</sup>H. Ni and X. Li, *Nanotechnology* **17**, 3591 (2006).

<sup>10</sup>W. Mai and Z. L. Wang, *Appl. Phys. Lett.* **89**, 073112 (2006).

<sup>11</sup>M. Lucas, W. Mai, R. Yang, Z. L. Wang, and E. Riedo, *Nano Lett.* **7**, 1314 (2007).

<sup>12</sup>G. Stan, C. V. Ciobanu, P. M. Parthangal, and R. F. Cook, *Nano Lett.* **7**, 3691 (2007).

<sup>13</sup>H. Ni, X. Li, and H. Gao, *Appl. Phys. Lett.* **88**, 043108 (2006).

<sup>14</sup>B. Wu, A. Heidelberg, and J. J. Boland, *Nat. Mater.* **4**, 525 (2005).

<sup>15</sup>M. Tortonese and M. Kirk, *Proc. SPIE* **3009**, 53 (1997).

<sup>16</sup>P. G. Laurson and W. J. Cox, *Mechanics of Materials* (Wiley, New York, 1967), Chap. 11, p. 194.

<sup>17</sup>W. C. Oliver and G. M. Pharr, *J. Mater. Res.* **7**, 1564 (1992).